Catena 159 (2017) 144–148

Contents lists available at ScienceDirect

Catena

journal homepage: www.elsevier.com/locate/catena

Coherent structures over flat sandy surfaces in aeolian environment

Zhen-Ting Wang[a,b,*], Chun-Lai Zhang[a], Hong-Tao Wang[b]

[a] State Key Laboratory of Earth Surface Processes and Resource Ecology, MOE Engineering Research Center of Desertification and Blown-sand Control, Beijing Normal University, Beijing 100875, PR China

[b] Northwest Institute of Eco-Environment and Resources, CAS, Lanzhou 730000, PR China

ARTICLE INFO

Keywords:
Coherent Structure
Sandy Surface
Wind Tunnel
PIV
POD

ABSTRACT

A basic assumption in many theoretical models of aeolian sediment transport is that airflow is uniform. In fact, turbulence is structural, and there exist extremely complex dynamic behaviors. Coherent structures are probably most important features. Nowadays aeolian researchers are generally aware of the significance of coherent structures, although even their basic forms have not been revealed completely. In the current research, the wind tunnel experiment with the help of the particle image velocimetry (PIV) technique and the proper orthogonal decomposition (POD) method shows that there are streamwise, elongated, low- and high-speed, streaks-type coherent structures over sandy surfaces with and without saltation in aeolian environment.

Boundary-layer turbulence is a traditional topic in fluid mechanics (Cebeci and Smith, 1974; Schlichting, 1979; Boiko et al., 2002). In this purely deterministic system (Tsinober, 2014), there are extremely complex dynamic behaviors often associated with mass and momentum transfer, energy conversion and dissipation. Coherent structures (or organized motions) are probably most important features (Robinson, 1991; Smits et al., 2011; Sharma and McKeon, 2013). According to Robinson (1991), a coherent motion can be defined as a three-dimensional region of the flow over which at least one fundamental flow variable (velocity component, density, temperature, *etc.*) exhibits significant correlation with itself or with another variable over a range of space and/or time that is significantly larger than the smallest local scales of the flow. Many coherent structures, *e.g.* high- and low-speed streaks, ejections, sweeps, and vortical structures of various forms, were identified and investigated in detail at low to moderate Reynolds numbers (Robinson, 1991). Four types of coherent structures, *i.e.* streaks, hairpin vortices, large-scale motions, and very-large-scale motions, were classified at high Reynolds numbers (Smits et al., 2011). Although significant achievements in coherent structures formed by pure fluid in boundary-layer flows have been made over the past decades, similar phenomena are still not well understood for fluid-particle transport which commonly occurs over the earth's surface. In aqueous environment, three known categories of coherent structures are streamwise vortices, hairpin vortices, and larger scale eddies (Mazumder, 2000). Their implications for sediment transport were also proposed (Mazumder, 2000; GYR, 2011). Whereas in aeolian environment, even the basic forms of coherent structures have not been revealed completely (Bauer et al., 2013). High-frequency records of wind velocity in field suggest that ejection-like and sweep-like events might exist over flat sandy surfaces (Bauer et al., 1998; Sterk et al., 1998; Ellis, 2006). As manifestations of coherent structures, aeolian streamers (also named as sand snakes) were regarded as the products of near-surface gusts due to down sweeps of large eddies from higher regions (Baas, 2003). A numerical work of large eddy simulations showed that aeolian streamers appear clearly related to elongated near-surface eddies (Dupont et al., 2013). Saltation intermittency was investigated in wind tunnel experiments (Wang et al., 2014; Carneiro et al., 2015). But the flow structures responsible for the intermittent process of mass transport are unclear.

In the current study, the methods of PIV and POD were jointly applied to detect coherent structures over sandy surfaces with and without saltation in a series of wind tunnel experiments.

The experiments were performed in an open-circuit wind tunnel with a 6.0*m* long, 1.0*m* wide, and 1.0*m* high working section. The detailed descriptions of the wind tunnel were given in our previous investigations of aeolian saltation by using high-speed photography (Wang et al., 2013, 2014). Both top surface and two sidewalls are made of clear glass, so that flow visualization and PIV measurements can be realized. The wind speed on the tunnel axis can be continuously changed from 2*m/s* to 45*m/s*. The bottom surface of working section was covered by the dry, loose, artificial sand with the mean diameter of $d = 450\mu m$ or $d = 800\mu m$ and a density of $2.65 \times 10^3 kg/m^3$. The 8*mm* thick sand bed was carefully smoothed using a straight wood bar with small uniform pressures prior to each test. The PIV systems produced by TSI company were used to acquire two instantaneous flow velocity components, *i.e.* streamwise and vertical components. The tunnel axis

* Corresponding author.
E-mail address: wangzht@lzu.edu.cn (Z.-T. Wang).

http://dx.doi.org/10.1016/j.catena.2017.08.011
Received 27 May 2017; Received in revised form 19 July 2017; Accepted 16 August 2017
Available online 30 August 2017

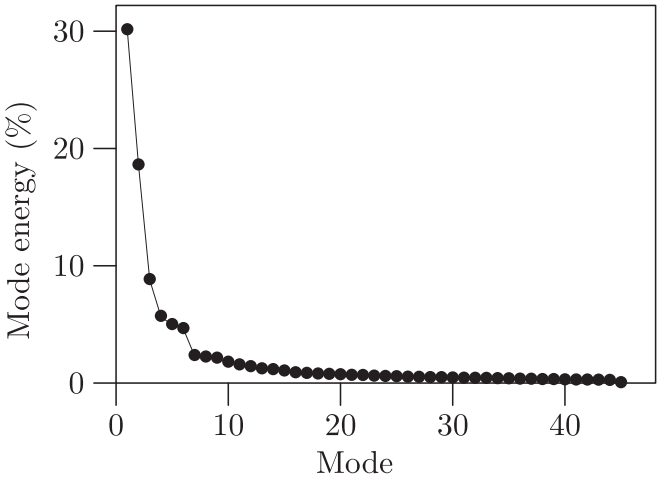

Fig. 1. Energy fraction of the individual POD modes. The sand diameter and the free-stream velocity on the tunnel axis are $d = 800\mu m$ and $u_\infty = 10.0m/s$, respectively.

was included in the plane of the green laser light sheet perpendicular to the sand bed. The camera was located $0.06m$ from the sidewall, and normal to the laser light sheet. Time separation between the two laser pulses was adjusted to $200 - 300\mu s$ for most free-stream velocities. Image dimension and spatial resolution were 4008×2672 pixels and $85.76\mu m$/pixel, respectively. The duration between two successive image pairs is $1.0s$. Given the above values of these control parameters, the maximum number of image pairs capable of being recorded by the camera is 15 in each test case. Talcum particles with the average diameter of $2\mu m$ were used for seeding. Given a free-stream velocity, the identical flow domain was investigated three times, *i.e.* 45 image pairs were obtained. All experiments were conducted at night to exclude the disturbance of sunlight, and the relative environmental factors, such as temperature and humidity, did not change significantly.

PIV is a sophisticated technique widely employed in many fields (Raffel et al., 2007). Here image analysis was carried out by using the open-source software of OpenPIV (Taylor et al., 2010). The available size of the interrogation window can be changed from $2^3 \times 2^3$ to $2^{10} \times 2^{10}$ pixels in the program. The smaller interrogation window is given, the more detailed flow field is recovered from PIV images. But the reconstructed flow field will be locally distorted and consequently become alienated from reality, if the interrogation window is too small. For the flow we measured, the streamwise velocity component is usually much larger than the vertical component. After performing a number of tentative calculations, we found that a rectangular interrogation window with the size of 128×64 pixels is competent for the flow field reconstruction. Another key factor in our PIV image analysis is the influence of solid parts including the sand bed and saltating grains. The immovable sand bed in images was cut and eliminated directly. According to Mie's scattering theory, the scattered light intensity increases with increasing particle diameter. Different from individual tracer particles, saltating grains are highly visible. Therefore, the vectors due to saltating grains were treated as outliers by the local filtering of OpenPIV. The disturbance of saltating grains also can be excluded from the raw images in advance. As done in the previous trajectory measurement (Wang et al., 2013), every saltating grain can be successfully distinguished. The major defect of this method is that the calculation is time-consuming.

Once velocity fields are obtained, an analytical method is required to look for coherent structures. A rich variety of tools has emerged from the study of fluid mechanics (Robinson, 1991). As far as we know, at least four methods, *i.e.* quadrant splitting (Sterk et al., 1998; Chapman et al., 2013), variable interval time average (Bauer et al., 1998), wavelet transform (Baas, 2006; Ellis, 2006), and conditional average (Jacob and Anderson, 2017), have been introduced into aeolian research. As an objective, unbiased, statistical technique that contributes to deterministic dynamical analysis, POD based on velocity or vorticity fields can effectively identify coherent structures from various flows (Berkooz et al., 1993; Gurka et al., 2006;Tang et al., 2015). We adopted the velocity-based rather than vorticity-based POD, so as to avoid data errors generated by vorticity which must be further computed in terms of the first order spatial derivative of velocity. The velocity field $\mathbf{u}$ can be approximately decomposed into the time-averaged component $\overline{\mathbf{u}}$ and the linear sum of a finite orthogonal set of spatial eigenfunctions $\mathbf{\Phi}_k$,

$$\mathbf{u}(\mathbf{x}, t) \approx \overline{\mathbf{u}}(\mathbf{x}) + \sum_{k=1}^{k=N} a_k(t)\mathbf{\Phi}_k(\mathbf{x}) \tag{1}$$

where $\mathbf{x}$ and t are space and time coordinates, N is the total number of POD modes, a_k is the corresponding coefficient of the POD mode $\mathbf{\Phi}_k$. It should be pointed out that coherent structures are not explicitly dependent of $\overline{\mathbf{u}}$. The second part in the right-hand side of Eq. (1) is an optimally spatial description of coherent structures containing most of energy of the fluctuating velocity field. POD modes are arranged in descending order according to their energy fractions. $\mathbf{\Phi}_k$ and a_k, representing coherent structure and energy contribution, were conveniently calculated by using the snapshot technique offered by the POD toolbox of OpenPIV. More detailed mathematical theory and computation procedures of the POD are referred to refs. (Sirovich, 1987; Berkooz et al., 1993).

In the low-Reynolds number flows we investigated, the energy fraction decreases with the sequence number of POD modes rapidly, as shown in Fig. 1. The first mode generally accounts for 20–40% of the total energy. So the first mode is accepted as the dominant coherent structure.

Figs. 2 and 3 show the first POD modes for the $450\mu m$ and $800\mu m$ sand beds. The direction of time-averaged velocity $\overline{\mathbf{u}}$ is from left to right. Inverted arrows, say those in Fig. 2 (c), indicate that some coherent structures are low-speed motions. From Figs. 2 and 3, one might conclude that the coherent structures in most cases are low-speed motions. This is just a coincidence. Actually, high-speed motions are predominant in many other flow conditions we measured. The influence of surface conditions is indistinct because the sand diameter is smaller compared to the spatial scales of these streamwise low- and high-speed coherent structures. For pure airflows (Figs. 2 (a) and 3(a)), coherent structures usually less than $2cm$ in width are very close to the surface. This is consistent with numerous previous reports on boundary-layer flows, see (Robinson, 1991) and references therein. When saltation is being initiated (Figs. 2 (b) and 3(b)), the scale of coherent structures can reach 5–10 cm in width. But they still maintain their position near the surface. When there are a quantity of saltating sand grains in the air, *e.g.* about 280 and 150 grains in the flows shown in Figs. 2 (c) and 3(c), coherent structures with widths of 3–5 cm occur in the height of 3–7 cm above the surface. Comparing with those in former cases, coherent structures become smaller in size, and some are tilted, as shown in Fig. 3 (c). The saltation layer could behave as roughness elements (Owen, 1964). We suppose that saltating grains restrict and influence the scale and direction of coherent structures in this case.